

Preparation and characterization of a novel bioactive bone cement: Glass based nanoscale hydroxyapatite bone cement

QIANG FU¹, NAI ZHOU¹, WENHAI HUANG^{1,*}, DEPING WANG¹,
LIYING ZHANG¹, HAIFENG LI²

¹*School of Materials Science and Engineering, Tongji University, Shanghai, 200092, P.R. China*

E-mail: whhuang@mail.tongji.edu.cn

²*Tongji Hospital Affiliated Tongji University, Shanghai, 200065, P.R. China*

A novel type of glass-based nanoscale hydroxyapatite (HAP) bioactive bone cement (designed as GBNHAPC) was synthesized by adding nanoscale hydroxyapatite (HAP) crystalline (20–40 nm), into the self-setting glass-based bone cement (GBC). The inhibition rate of nanoscale HAP and micron HAP on osteosarcoma U2-OS cells was examined. The effects of nanoscale HAP on the crystal phase, microstructure and compressive strength of GBNHAPC were studied respectively. It was concluded that nanoscale HAP could inhibit the cell proliferation, while micron HAP could not, and that nanoscale HAP could be dispersed in the cement evenly and the morphology did not change significantly after a longer immersion time. XRD and FTIR results show nanoscale HAP did not affect the setting reaction of the cement. Furthermore, GBNHAPC had a higher compressive strength (92 MPa) than GBC. It was believed that GBNHAPC might be a desirable biomaterial that could not only fill bone defects but also inhibit cancer cell growth.

© 2004 Kluwer Academic Publishers

1. Introduction

The repair of bone defects, where cancer tumors are removed, has been a difficult problem. It was reported that the reoccurrence rate of cancer cells in bone defects after tumorotomy operation could reach 8–40% [1, 2]. Bone cement was typically used as a delivery vehicle for antibiotics and anticancer drug for defect repair and bone diseases treatment. Conventional Polymethylmethacrylate (PMMA) bone cement has recently been replaced by inorganic self-setting calcium phosphate cement (CPC), because of the low biocompatibility and the associated toxicity of its degraded products [3]. Thus studies on CPC as a novel device for drug delivery system have attracted great deal of attention. Anticancer drugs are introduced into CPC with the aim of both repairing bone defects and inhibiting cancer cell growth [4]. However, the addition of anticancer drugs affected the setting reaction of CPC and the mechanical properties as well [5]. Therefore, only a limited number of anticancer drugs can be added to CPC. Furthermore, CPC has adverse effect on the proficiency of such anticancer drugs. All these make it hard for CPC to be widely accepted as a desirable drug release system. Glass based bone cement (GBC) has been reported to possess high biocompatibility and mechanical strength

[6, 7] but few studies have been reported on its drug release property. Therefore, the development of a new type of bone cement that possesses not only a high mechanical strength but also an ability to inhibit cancer cell from reproduction, has become an intense focus in medical and material fields.

Hydroxyapatite (HAP, $\text{Ca}_{10}(\text{PO}_4)_6(\text{OH})_2$) is a most suitable material for bone defects repair because of its excellent biocompatibility. The latest research shows that nanoscale HAP crystallite could inhibit the growth of certain kinds of cancer cells, while having little side effects on normal cells [8, 9]. This, undoubtedly, could result in a new method for treatments of bone disease. However, the mechanical strength of HAP crystallite is so low that it can not form a fixed shape in human body, which hinders the clinical application of nanoscale HAP crystallite. When added to CPC, nanoscale HAP crystallite will grow during the setting reaction of CPC. Eventually its nanoscale characteristics and the ability to inhibit cancer cell growth disappear.

In this paper, the effects of nanoscale HAP and micrometer HAP on a bone cancer cell, U2-OS, growth were studied. Two composites were synthesized by adding nanoscale HAP and micrometer HAP into glass bone cement respectively. The mechanical properties of

*Author to whom all correspondence should be addressed.

the two composites were studied. Moreover, the crystal phase and microstructure of the glass based nanoscale HAP bone cement (designated GBNHAPC) were also characterized.

2. Materials and methods

2.1. Materials

Glass composition was designed on consideration of a self-setting $\text{Ca}_3(\text{PO}_4)_2$ and CaSiO_3 crystals, which possessed a high mechanical strength. With respect to the preparation process and the properties of the final glass, glass with a nominal composition of CaO 45, SiO_2 35, and P_2O_5 20 by weight ratio was selected. Glass batch was melted in an SiC furnace at 1500°C for 4–6 h. The melt was quenched into glass between stainless plates, and then the glass was crushed and pulverized in an aluminum-ball mill into fine powder (3 to $5\ \mu\text{m}$).

Nanoscale HAP crystallite was developed through a wet-chemistry method using $\text{Ca}(\text{NO}_3)_2$ and $(\text{NH}_4)_2\text{HPO}_4$ with the molar ratio of calcium to phosphate was maintained 1.67. $(\text{NH}_4)_2\text{HPO}_4$ solution was slowly added to $\text{Ca}(\text{NO}_3)_2$ solution to produce HAP sol. After aging for 24 h, HAP sol was filtered and washed several times. The sol was dried in an oven for a certain time and then as-dried HAP was milled. The particles produced were spherical HAP crystallite with the average size of 20–40 nm. Micron HAP, with the average size of 1–4 μm , was purchased from Shanghai Medicine corporation.

$(\text{NH}_4)_2\text{HPO}_4$ and $\text{NH}_4\text{H}_2\text{PO}_4$ with analytical reagent grade were dissolved in deionized water at a certain ratio to get an solution with a pH value of 7.4.

Bioactive bone cement was produced by mixing the powder (glass powder and nanoscale HAP crystallite or micron HAP) with the ammonium phosphate medium evenly. The specimens were immersed in simulated body fluid (SBF) at 37°C . The SBF solution is the closest to human plasma, as shown in Table I.

2.2. Methods

Compressive strength of bone cement, composed of nanoscale HAP or micron HAP and glass powder, was measured using an Instron universal testing machine (Instron 1195, Instron Limited, Buckinghamshire, UK) at a crosshead speed of 0.5 mm/min. Rectangular beams (7 mm \times 7 mm \times 12 mm) were prepared and measured under wet conditions at room temperature after immersing in SBF at 37°C for 7, 15 and 30 days respectively. For each time interval, at least 5 specimens were tested to get a mean value.

Morphology of as-dried HAP crystallite was observed using TEM (H600, Hitachi, Tokyo, Japan) and microstructure of the bone cement was observed using

field emission scanning electron microscopy (Hitachi JSM-6700F, Hitachi, Japan). The crystal phase of the cement was analyzed by XRD (D/max 2550v, Rigaku Co., Tokyo, Japan) and FTIR (FTS-40 BIORAD, Digilab Division, Cambridge, MA).

2.3. Cell proliferation

Osteosarcoma U2-OS cells were obtained from Institute of Cell Biology of Chinese Academy of Science (Shanghai, China). U2-OS cells (3000 cell/ml) were cultured in RPMI medium 1640 (Gibco, USA) supplemented with 10% fetal bovine serum (FBS, Gibco, USA), 2 mM glutamine, 1 mM sodium pruvate, $100\ \text{U ml}^{-1}$ of penicillin, $100\ \mu\text{g/ml}$ of streptomycin and $50\ \mu\text{g/ml}$ of ascorbic acid. U2-OS cells were plated into 96-well culture plate, 0.2 ml in each well, maintained at 37°C in a fully humidified atmosphere at 5% CO_2 in air for 24 h. Then the medium in control groups was replaced by fresh medium and medium in the trial groups was replaced by nanoscale HAP suspension and micrometer HAP suspension respectively. Suspensions ($250\ \mu\text{g/ml}$) were made by mixing nanoscale HAP or micrometer HAP with the RPMI medium 1640 respectively.

Cell proliferation was measured using the MTT (3-[4,5-dimethyl-2-thiazolyl]-2,5-diphenyl-2H tetrazolium-bromide, Merk, Schuchardt, Germany) test. Cell proliferation was determined at 1, 2 and 3 days. The medium was removed and 0.2 ml MTT solution was added to each well. Following incubation at 37°C for 4 h in a fully humidified atmosphere at 5% CO_2 in air, the untransformed MTT was removed and 0.3 ml of isopropanol were added, the optical density was measured using ELISA (Enzyme-linked immunosorbent assays) reader (EL311SX, AutoReader, Bio-Tek Instruments, Winooski, VT) at a wavelength of 570 nm.

The inhibition rate of nanoscale HAP or micrometer HAP was assessed by the following formula:

$$\frac{\text{Trial group OD value} - \text{control group OD value}}{\text{Control group OD value}} \times 100\%$$

Three samples for each material or control were randomly processed for scanning electron microscope (SEM): cells grown on the material were fixed in 2.5% glutaraldehyde, in pH 7.4 phosphate buffer 0.01 M for 1 h, and dehydrated at a graded ethanol series. Then, samples were washed four times in liquid CO_2 and submitted to critical point dehydration in CO_2 atmosphere (80 atm at 33°C). Finally, the samples were mounted on aluminium stubs for SEM analysis, earthed with silver glue and then metallised with a thin film ($25\ \text{\AA}$)

TABLE I Ion concentration (mM) in SBF and in human blood plasma [10]

| Ion | Na^+ | K^+ | Mg^{2+} | Ca^{2+} | Cl^- | HCO_3^- | HPO_4^{2-} | SO_4^{2-} |
|--------------|---------------|--------------|------------------|------------------|---------------|------------------|---------------------|--------------------|
| SBF | 142.0 | 5.0 | 1.5 | 2.5 | 147.8 | 4.2 | 1.0 | 0.5 |
| Human plasma | 142.0 | 5.0 | 1.5 | 2.5 | 103.0 | 27.0 | 1.0 | 0.5 |

with Au-Pd. The stubs were examined at 20 KV with a current of 60 μ A on SEM.

3. Results and discussion

3.1. Effect of nanoscale HAP on osteosarcoma U2-OS cells

The effects of nanoscale HAP and micron HAP on osteosarcoma U2-OS cells proliferation was investigated and the results were shown in Table II.

It could be seen from Table II that nanoscale HAP has a greater effect on U2-OS cell proliferation than micron HAP. The inhibition rate of nanoscale HAP grows with the time and reaches 73% after 3 days.

In order to study the morphology changes of U2-OS cells, three samples were observed using SEM, shown in Fig. 1.

It was seen that in the control group (Fig. 1(a)) the cells grew well and all the cells possessed a shape. In Fig. 1(b), although they grew quite well, some particles appeared in the cells. In Fig. 1(c), the morphology of the cells changed greatly compared with that of (a) and (b). The sizes of the cells differed from one to another and the shape changed from a shape to a spherical or elliptical shape. Most of the cells showed the trend of being poisoned by nanoscale HAP particles.

3.2. Compressive strength analysis

The compressive strength of bone cement, composed of nanoscale HAP or micron HAP and glass powder, after different immersion time in SBF was measured. The results are shown in Fig. 2.

It could be seen that the compressive strength of three bone cement- GBC, GBNHAPC and glass bone cement with micron HAP—increased with a longer immersion time. Fig. 2 also shows that the bone cement with nanoscale HAP reached the highest compressive strength, while the cement with micron HAP the lowest compressive strength.

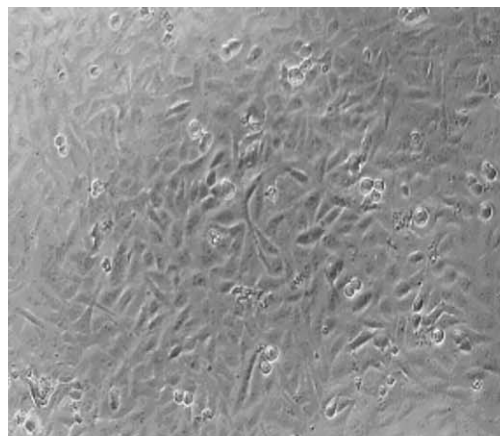
3.3. Crystal phase analysis

Samples of different immersion time in SBF were analyzed using XRD. Figs 3 and 4 show XRD spectra of GBC and GBNHAPC at different immersion time respectively.

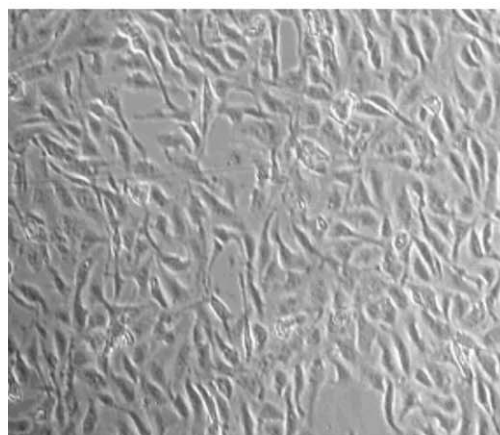
Both figures indicate that with the increasing of immersion time, XRD peaks of the two cements became sharper and narrower. They also show that a certain amount of primary HAP crystal has occurred after immersing for 7 days. With the proceeding of immersion,

TABLE II Inhibition rate (%) of nanoscale HAP and micron HAP on osteosarcoma U2-OS cells

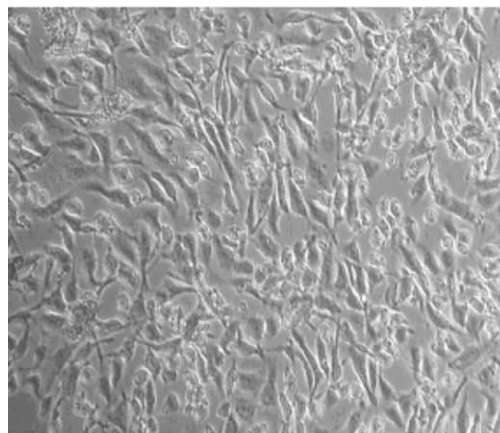
| Groups | Time/day | | |
|---------------|----------|----|----|
| | 1 | 2 | 3 |
| Micron HAP | 37 | 28 | 21 |
| Nanoscale HAP | 41 | 56 | 73 |



(a)



(b)



(c)

Figure 1 Morphology of U2-OS cells in different culture medium: (a) pure culture medium; (b) culture medium with micron HAP and (c) culture medium with nanoscale HAP.

the crystal structure of HAP generated by GBNHAPC and GBC tended to consummate and also the size of primary HAP grew larger. Compared Fig. 3 with Fig. 4, it was clear that XRD peaks of GBNHAPC were sharper than that of GBC and the intensity was also higher. This was due to nanoscale HAP crystallite that was doped in GBNHAPC. The dopant resulted in the sharpening of the XRD peaks of GBNHAPC.

Functional groups in GBC and GBNHAPC were analyzed using FTIR, shown in Fig. 5. It can be seen from Fig. 5 that functional groups in both cements are

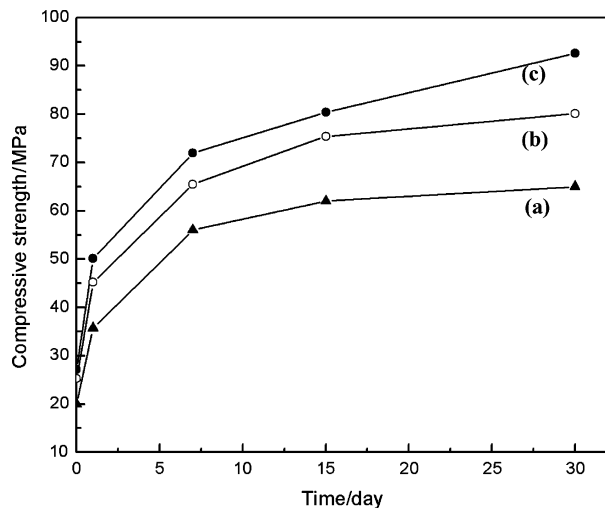


Figure 2 Compressive strength of bone cement after different immersion time: (a) glass bone cement with micron HAP; (b) GBC and (c) GBNHAPC.

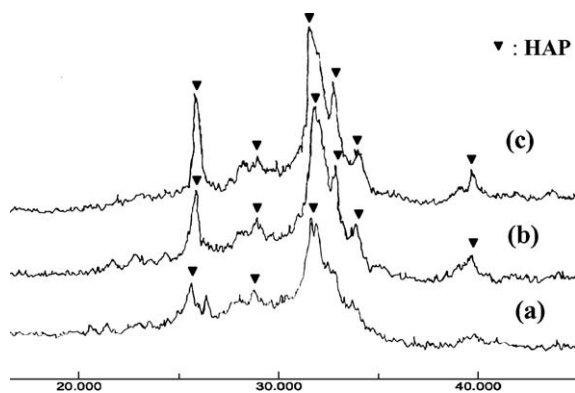


Figure 3 XRD spectra of GBC after different immersion time: (a) 7 days; (b) 15 days and (c) 30 days.

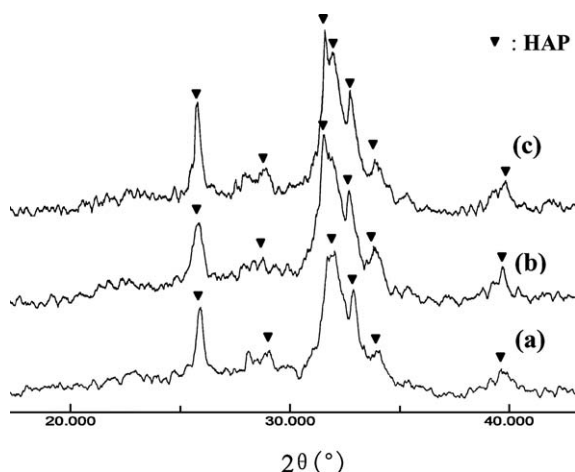


Figure 4 XRD spectra of GBNHAPC after different immersion time: (a) 7 days; (b) 15 days and (c) 30 days

the same. Peaks of 1420 cm^{-1} and 1450 cm^{-1} corresponded to the splitting and entrance of CO_3^{2-} groups into HA crystal. Peaks of 560 cm^{-1} and 602 cm^{-1} corresponding to the bending vibration of crystal P—O bond and 1080 cm^{-1} corresponding to the stretching vibration of P=O bond indicate the formation of hydroxy-carbonate apatite (HCA) in GBC [11]. The peak of 464 cm^{-1} corresponding to the metamorphosis vibra-

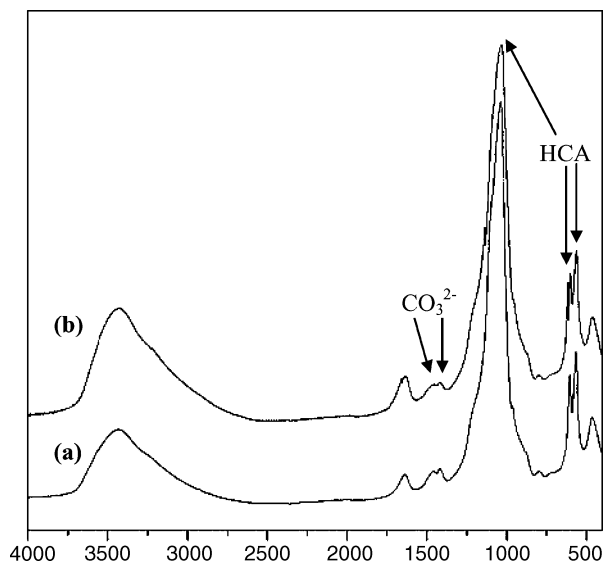


Figure 5 FTIR spectra of bone cement after 7 days immersion time; (a) GBC and (b) GBNHAPC.

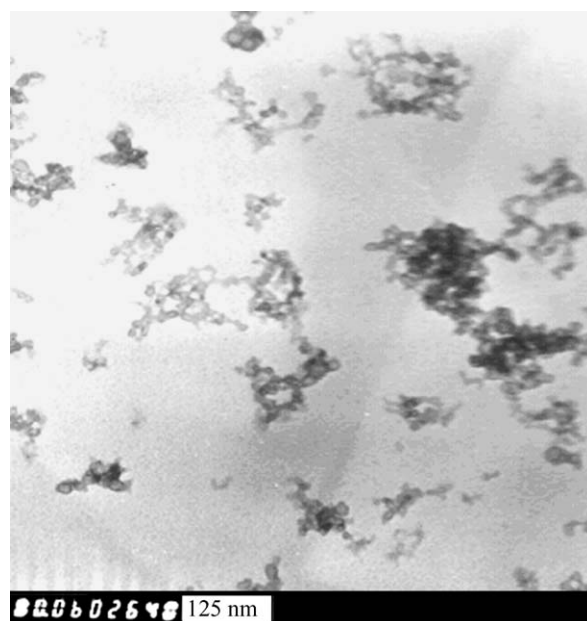


Figure 6 TEM pictures of as-dried nanoscale HAP crystallite.

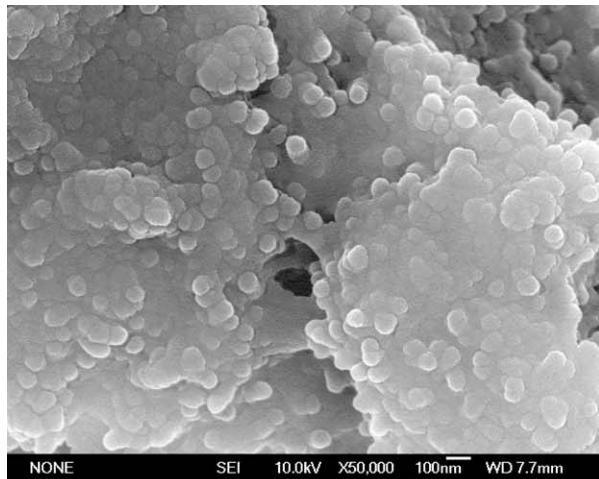
tion of O—Si—O indicates the appearance of the SiO₂-rich layer in GBC.

3.4. Microstructure

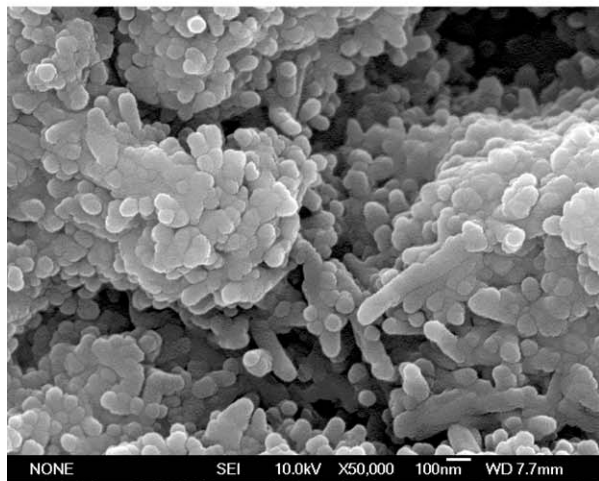
Nanoscale HAP synthesized in the experiment was observed under TEM (see Fig. 6). It could be seen from the graph that HAP in GBNHAPC was nanoscale HAP crystallite with a spherical shape, with the sized ranged from 20 nm to 40 nm.

The scatterance and change of the morphology of nanoscale HAP in GBNHAPC samples immersed in SBF for 7, 15 and 30 days respectively were observed under SEM.

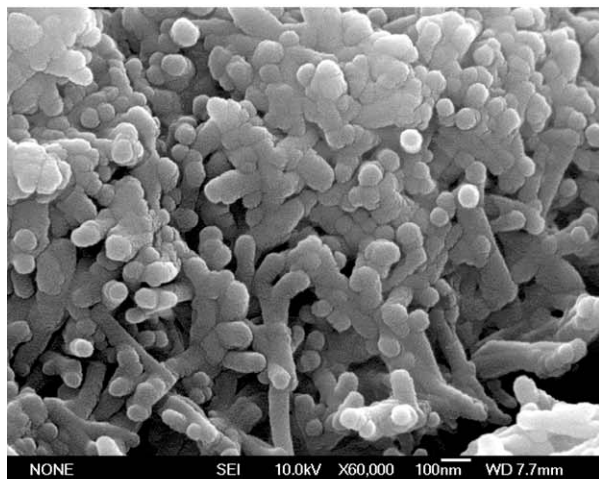
Fig. 7 shows different microstructure of these three samples. It indicates that nanoscale HAP crystallite were dispersed homogenously among glass powder. After 7 days nanoscale HAP was observed to scatter between the interfaces of glass powder. And little primary



(a) 7days



(b) 15 days



(c) 30 days

Figure 7 SEM pictures of GBNHAPC samples obtained after different immersion time.

HAP produced by glass powder was observed. The size of nanoscale HAP remained at 20–40 nm. After 15 days and 30 days, a great number of primary needle-like primary HAP crystals were observed to be generated from the surface of glass powder and scatter between powder interfaces with the nanoscale HAP crystallite entangled with them. Furthermore, with a longer immersion time, the primary HAP crystals formed from

glass powder increased in length and reached 200–300 nm after 30 days (see Fig. 7(c)). A chemical bond occurred between the nanoscale HAP crystallite and the primary needle-like HAP crystals, resulting in the increase of the mechanical strength and the density of GBNHAPC. It could be seen from Fig. 7 that a compact network structure was eventually formed after 30 days, which indicates that the synthesis of nanoscale HAP crystallite might promote the hydration reaction of GBC.

It could be concluded that a longer immersion time in SBF had little effect on the morphology of nanoscale HAP and the granularity of it still ranged from 20 nm to 40 nm.

4. Discussion

An ideal biomaterial for bone defects repairing after tumorotomy operation should be able to inhibit the cancer cell growth around the defects, as well as bearing load from the body. Great efforts have been concentrated on the drug delivery system using CPC or GBC as a medium [12, 13]. This system, by carrying antibiotic drugs in cement, can inhibit certain kind of cancer cells growth. However, due to the disturbance of the drugs on the hydration reactions of the cement, the mechanical strength, crystal phase and microstructure are greatly affected. Especially, the mechanical strength decreased greatly. In this study, we examined the effects of nanoscale HAP and micron HAP on the osteosarcoma U2-OS cells proliferation, compared the mechanical strength of cement containing nanoscale HAP and micron HAP, and studied the crystal phase and microstructure of the bone cement containing nanoscale HAP. Our results showed that nanoscale HAP was more effective for the inhibition of a certain kind of bone cancer cells, osteosarcoma U2-OS cells and that the mechanical strength of GBNHAPC was also much greater than that of GBC or bone cement containing micron HAP.

Previous work has showed that nano HAP could inhibit the proliferation of such cancer cells as liver, paunch and throat cancer cells [8, 9]. Yet, no results concerning the effects of nanoscale HAP on bone cancer cells proliferation have been reported. In our work, we choose a regular cancer cell, osteosarcoma U2-OS cell, for our experiments and micron HAP as a control group for nanoscale HAP. Our results revealed that the inhibition rate of nano HAP on osteosarcoma U2-OS cell increased with time, while that of micron HAP decreased greatly. As calmodulin (CaM) at the cancer cells surfaces was several times higher than at the normal cells surfaces, the proliferation of cancer cells tended to be affected by calcium ion concentration around them. Therefore, calcium ion released from nano HAP and micron HAP may result in the more absorption of calcium ion into cancer cells, leading to the lower growth rate. Furthermore, nanoscale HAP ranged from 10–50 nm and micron HAP differs greatly in chemical and physical properties, for example, a higher solubility, surface energy, ion exchange capability and polarization. This made it easier for nanoscale HAP to react with the cancer cells surfaces or even to enter

the cells, reacting with the inner parts of them. Therefore, the cancer cells growth was greatly inhibited by nanoscale HAP.

Our work also showed that GBNHAPC had the highest mechanical strength in the three bone cements (GBC, GBNHAPC and bone cement containing micron HAP) and that the hydration reaction of the cement was not affected by nano HAP, which could be inferred from the similarity of the crystal phase, shown in Figs 3–5. The SEM picture of the microstructure of GBNHAPC indicates that the morphology of the added nanoscale HAP in bone cement did not change greatly, which guaranteed the inhibition ability of it on cancer cells.

5. Conclusion

In summary, the effect of nanoscale HAP on cancer cells proliferation was examined, a new bone cement composed of glass powder and nanoscale HAP was synthesized and the mechanical strength, crystal phase and microstructure were investigated. Our study shows that nanoscale HAP had a notable inhibition on U2-OS cells proliferation and could enhance the mechanical strength of glass bone cement, while having little effect on the hydration reaction of the cement.

Acknowledgments

The authors are grateful to Dr Yongren Ben Peng at XL Sci-Tech, Inc. (Richland, WA) for his warmhearted discussion. And the authors would like to express their thanks to the Chinese Nature Science Foundation (NSF grant number 50272041) and the Nanotechnology Spe-

cial Foundation of Shanghai Science and Technology Committee (grant number 0144NM064) for their financial support.

References

1. M. CAMPANACCI, N. BALDINI and S. BORIANI, *J. Bone Joint Surg(Am)* **69**(1) (1987) 106.
2. S. A. BINI, K. GILL and J. O. JOHNSON, *Clin Orthop.* **321** (1995) 245.
3. W. J. MALONY, M. JASTY, A. ROSEMBERG and W. H. HARRIS, *J. Bone Joint Surg.* **72-B** (1990) 966.
4. C. HAMANISHI, K. KITAMOTO, S. TANAKA, M. OTSUKA and Y. DOI, *J. Biomed. Mater. Res.* **33** (1996) 139.
5. M. OTSUKA, Y. MATSUDA, Y. SUWA, J. L. FOX and W. L. HIGUCHI, *J. Pharm. Sci.* **83**(2) (1994) 259.
6. J. TAMURA, K. KAWANABE, M. KOBAYASHI, T. NAKAMURA, T. KOKUBO, S. YOSHIHARA and T. SHIBUYA, *J. Biomed. Mater. Res.* **30**(1) (1996) 85.
7. S. SHINZATO, T. NAKAMURA, J. TAMURA, T. KOKUBO and Y. KITAMURA, *ibid.* **56** (2001) 571.
8. S. ZHANG, S. LI and F. CHEN, *J. Wuhan University of Technology* **18**(1) (1996) 5.
9. H. AOKI, M. OGAKI and S. KANO, *Reports of Institute for Medical and Dental Eng.* **27**(1) (1993) 39.
10. T. KOKUBO, H. KUSHITANI, S. SAKKA, T. KITSUGI and T. YAMAMURO, *J. Biomed. Mater. Res.* **24** (1990) 721.
11. O. FILHO, LA TORRE and L. HENCH, *ibid.* **30**(4) (1996) 509.
12. M. BOHNER, J. LEMAÎTRE, P. VAN LANDUYT, P. Y. ZAMBELLI, H. P. MERKLE and B. GANDER, *J. Pharm. Sci.* **86** (1997) 565.
13. M. OTSUKA, M. SAWADA, Y. MATSUDA, T. NAKAMURA and T. KOKUBO, *Biomaterials* **18**(23) (1997) 1559.

Received 8 October 2003
and accepted 20 May 2004